THE PUBLISHING HOUSE
OF THE ROMANIAN ACADEMY

PROCEEDINGS OF THE ROMANIAN ACADEMY, Series A,
Volume 23, Number 2/2022, pp. 135–141

ATMOSPHERIC PRESSURE DISCHARGE WITH TWIN POWER-ELECTRODES AND A DIELECTRIC WITH GRADED PERMITTIVITY ALONG THE SURFACE

Zelin ZHANG

Shanxi University, Department of electric engineering and architecture
E-mail: 202023504044@email.sxu.edu.cn

Abstract. The non-equilibrium plasma with atmospheric pressure shows a significant potential application in surface modification of materials, and the influence of the barrier material on dielectric barrier discharge (DBD) has been drawing attention in recent years. In this paper, we report a two-dimensional fluid model combined with twin power-electrodes, in order to investigate the properties of negative streamer produced by dielectric barrier discharge with graded dielectric barrier permittivity. The electrical parameters, electron density distribution and surface charge accumulation are studied. It is demonstrated that the discharge process will be softly and continuously changed. The application of graded material shows a potential as a barrier in dielectric barrier discharge.

Key words: dielectric barrier discharge, twin power-electrodes, variable permittivity.

1. INTRODUCTION

Material surface modification with atmospheric dielectric barrier discharge has been being the focus of intersection with both dielectric barrier materials and discharge [1]. Surface fluorination by low-temperature plasma treatment is proved to be a useful method to improve surface electrical strength of insulating materials [2]. It is reported that nitrogen functional groups and a large number of oxygen functional groups on the surface of carbon fiber fabrics can be introduced by glow discharge plasmas at low discharge voltage [3]. It is well known that the characteristics of dielectric barrier discharge (DBD) are dominantly by the factors including electric field distribution and voltage applied. The electric field can be easily adjusted by variable permittivity, making it a convenient and potential way in the applications. The discharge is more intense when the dielectric barrier with greater permittivity is applied [4, 5]. On the other hand, greater permittivity will result in higher surface charge density [6], and different surface charge density can change the electric field distribution. Besides, it is reported that a functionally graded material with nonlinear permittivity distribution is made by using 3D printing technology, which can create a gradient electric field on the dielectric barrier surface [7]. With the development of functionally graded material, it shows a potential way to adjust the plasma characteristics parameters in DBD [8]. Because of the higher efficiency and increased area affected, electrode-arrays have been implemented [9–11]. However, the influence mechanism of variable permittivity on the DBD, especially under the condition that multi-electrodes arrangements introduced, is still an unclear issue.

In this work, a two-dimensional fluid model is developed to study DBD with twin power-electrodes and graded permittivity dielectric barrier material. The spatiotemporal distributions of electron density and electric field are studied as streamers propagating. What's more, the effect of graded permittivity on co-propagating streamers' coalescence phenomenon is investigated as well.

2. COMPUTATIONAL MODEL

Fig. 1 shows a simplified two-dimensional model of the material surface treatment by introducing twin power-electrodes. The simulation domain is 3 mm (length) × 4.5 mm (height) Cartesian *x–y* coordinates. The

grounded electrode is underneath the dielectric, all along its length. The exposed twin power-electrodes are placed above the dielectric, the length of them are 0.5 mm and the radius of head 250 μm. The top side of the dielectric barrier is curved representing local material with rough surface. The continuity equation in this 2D model for all reactive and neutral species is Eq. (1).

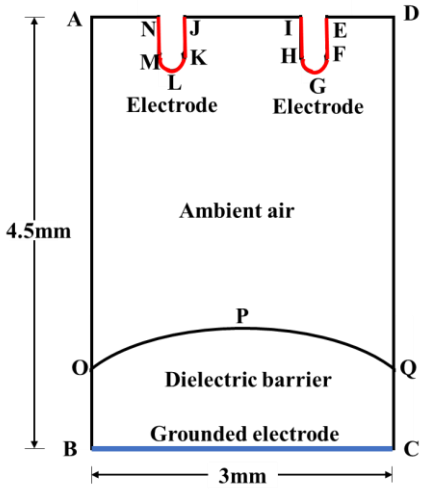

Fig. 1 – Schematic of the geometry of the dielectric barrier discharge with twin electrodes.

Both drift and diffusion for charged particles, Eqs. (2) and (3); diffusion for neutral particles is calculated by Eq. (4), in accord with Ref. [12]

$$\frac{\partial n_j}{\partial t} + \nabla \cdot \boldsymbol{j}_j = S_j \tag{1}$$

$$\boldsymbol{j}_{e,-} = -\mu_{e,-} \boldsymbol{E} n_{e,-} - D_{e,-} \nabla n_{e,-} \tag{2}$$

$$\boldsymbol{j}_{+} = \mu_{+} \boldsymbol{E} n_{+} - D_{+} \nabla n_{+} \tag{3}$$

$$\boldsymbol{j}_m = -D_m \nabla n_m , \tag{4}$$

where e, $-$, $+$ and m represent electrons, negative ions, positive ions and neutral species. n is the number density, in cm^{-3}, and $\boldsymbol{j}$ is the flux, in $cm^{-3}s^{-1}$. $\boldsymbol{E}$ is the electric field vector, μ is mobility, D is the diffusion coefficient, S_j is the source of species of species j (j = e, $-$, $+$), which can be derived from the chemical reactions. The working gas is simplified as 80% N_2 and 20% O_2. The species and reactions in the model are given in Ref. [12]. The rate coefficients of electron impact reactions are obtained by solving Boltzmann's equation using BOLSIG+ [13]. Cross sections are taken from the Morgan, TRINITI, and Phelps databases [14]. What's more, the local field approximation is applied when calculating parameters, and the electron mean energy, electron transport coefficient are given as functions of reduced electric field.

The electric field is calculated by the Poisson equation [12]:

$$\nabla \cdot (\varepsilon_r \nabla \varphi) = -\rho / \varepsilon_0 , \tag{5}$$

where φ is the electric potential and ρ is the sum of the space charge density and the surface charge density, ε_0 is the vacuum permittivity. ε_r is the relative permittivity of dielectric barrier. The main plasma parameters including dielectric surface charge are calculated in this work:

$$\frac{\partial \sigma_s}{\partial t} = -e\left[\left(\sum \boldsymbol{j}_{+} - \sum \boldsymbol{j}_{-} - \boldsymbol{j}_e\right)\right) \cdot \boldsymbol{n}\right] \tag{6}$$

$$\boldsymbol{j}_e \cdot \boldsymbol{n} = \left(-\mu_e \boldsymbol{E} n_e - \gamma \sum j_{+}\right) \cdot \boldsymbol{n} \tag{7}$$

$$\boldsymbol{j}_{\pm} \cdot \boldsymbol{n} = \left(\mu_{\pm} \boldsymbol{E} n_{\pm} - D_{\pm} \nabla n_{\pm}\right) \cdot \boldsymbol{n}, \tag{8}$$

where $\boldsymbol{n}$ is the unit vector perpendicular to the dielectric surface, γ is the secondary emission coefficient, $\gamma = 0.01$. The secondary emission electron energy is set to 2.5eV.

The boundary conditions are given in Table 1,

Table1

Boundary conditions on potential φ and species density (n_e, n_+, n_-) in Fig. 1

NO.	n_e	n_+	n_-	**Potential** $\boldsymbol{u}$
BC	0	0	0	0
NMLKJ, IHGFE	0	0	0	V_a
OPQ	Eq. (7)	Eq. (8)	Eq. (8)	…
AN, JI, ED	$\frac{\partial n_e}{\partial x} = 0$	$\frac{\partial n_+}{\partial x} = 0$	$\frac{\partial n_-}{\partial x} = 0$	$\frac{\partial \varphi}{\partial x} = 0$
AB, CD	$\frac{\partial n_e}{\partial y} = 0$	$\frac{\partial n_+}{\partial y} = 0$	$\frac{\partial n_-}{\partial y} = 0$	$\frac{\partial \varphi}{\partial y} = 0$

where n_e, n_+ and n_- are the electron density, positive ions density and negative ions density, respectively; l is the distance along the OPQ, V_a is the applied voltage as shown in Fig. 2.

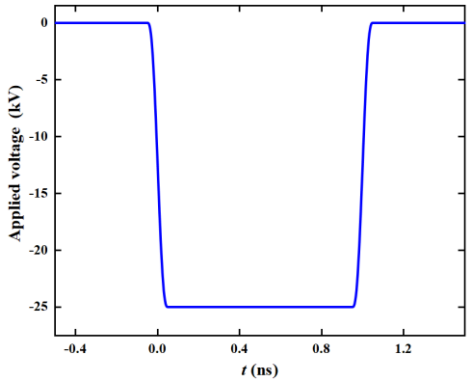

Fig. 2 – Voltage pulse applied to the powered electrode during DBD operation.

The pulsed DC voltage is –25 kV, and the rising time is 0.1 ns. The width of the pulse is 1 ns.

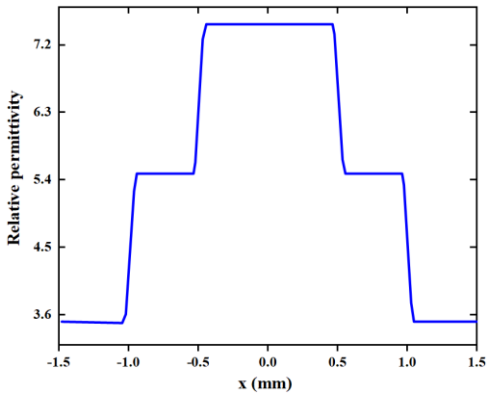

Fig. 3 – Graded permittivity ε_p distribution of dielectric barrier along the x direction.

As is depicted in Fig. 3, the practical graded permittivity ε_p is given as a function of x coordinate along the dielectric barrier surface. Obviously, non-linear distribution as a function of length along x direction is introduced. To be a comparison, the case of uniform distribution of dielectric permittivity under the condition of $\varepsilon_r = 7.5$ is studied as well.

The initial electron distribution is given by [15–17]:

$$n_e = N_{\max} \exp\left(-\frac{(x-x_1)^2 + (y-y_1)^2}{2\sigma^2} - \frac{(x-x_2)^2 + (y-y_2)^2}{2\sigma^2} \right), \tag{9}$$

where $N_{\max} = 10^{16}\ \mathrm{m}^{-3}$, $\sigma = 62.5\ \mu\mathrm{m}$. (x_1, y_1) and (x_2, y_2) are the spatial coordinates of needle electrodes head.

3. RESULTS AND DISCUSSION

As is shown in Fig. 4, the co-streamers in both uniform permittivity and graded permittivity introduced in the dielectric barrier have the trend to coalesce (two branches coalesce into one) during the propagation. Above the dielectric barrier with uniform permittivity, it depicts a higher electron density along the streamer path, and the streamers coalesce within a short time, resulting in a much wider range of spatial distribution of electron density. Once the channels are connected, as shown in Figs. 4c and 4d, the streamers will then charge the space near the dielectric barrier dramatically, this might be beneficial to the medical application, for example, plasma sterilization [18]. Meanwhile, it brings damage to the surface structure of dielectric barrier. Material surface modification needs less charge density on the dielectric barrier surface, especially when dealing with a layer of film on the surface. Compared (d) with (h) in Fig. 4, with graded permittivity dielectric introduced, the coalescence time of co-streamers is delayed. In fact, the electrons travel with a longer time spatially, fully colliding with various neutral molecules in the air. The same thing is that before the channels of co-streamers are connected, the streamers propagate with an almost the same speed above the dielectric barrier with both uniform permittivity and graded permittivity. The main reason may be found in the electric field distribution, as depicted in Fig. 5.

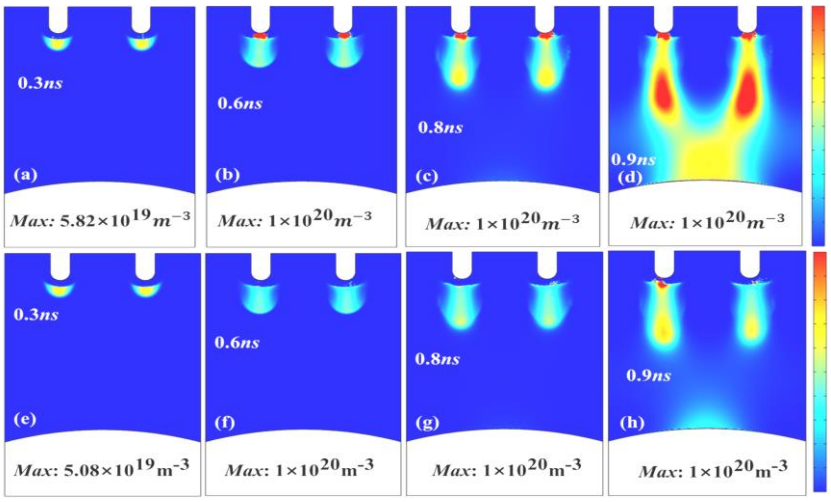

Fig. 4 – Distribution of electron density at different times with uniform permittivity $\varepsilon_r = 7.5$ (a), (b), (c) and (d), and graded permittivity ε_p (e), (f), (g), (h).

Figure 5 shows the evolution of electric field distribution during the streamer propagation. Before 0.9 ns, the magnitude of electric field rises slowly. At 0.9 ns, the pulsed voltage falloff, the magnitude of electric field spatially with graded permittivity dielectric barrier falls down to 6.07×10^7 V/m. This indicates that dielectric barrier with graded permittivity is sensitive to the variation of the voltage applied. This can provide a potential and faster way of accurate adjustment on the plasma parameters. The falling of the electric field magnitude results in slower propagation speed of co-streamers, and less surface charge density. Thus, the connecting time of propagating channels is delayed.

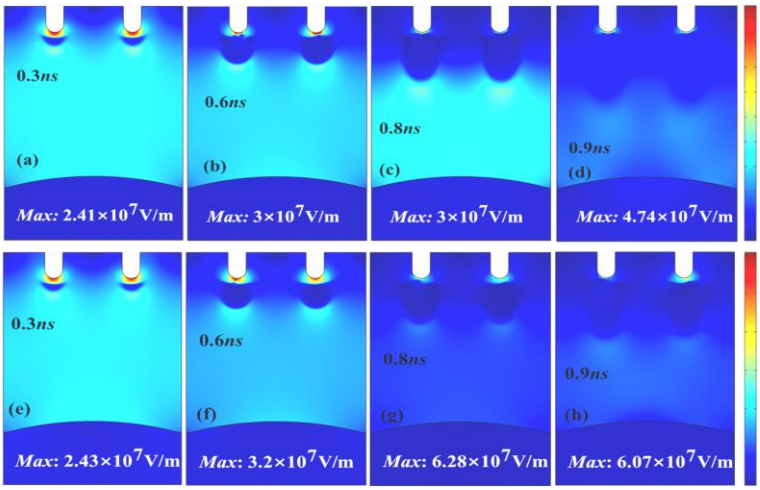

Fig. 5 – Electric field for a plasma streamer above the dielectric barrier with uniform permittivity (a), (b), (c), (d) and graded permittivity (e), (f), (g), (h).

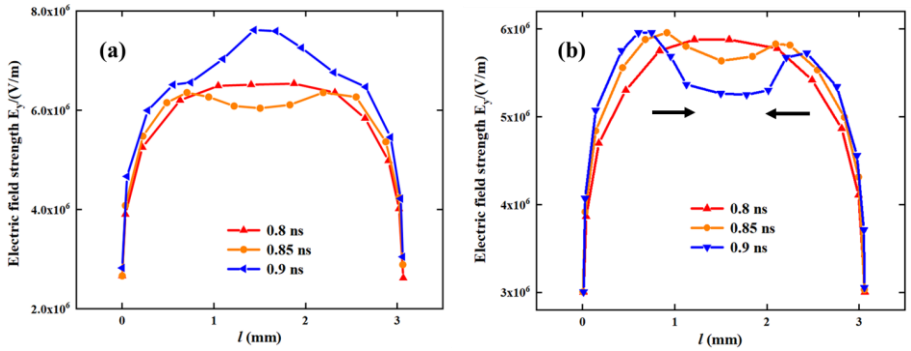

Fig. 6 – Electric field strength of E_y component above the dielectric barrier with uniform permittivity (a) and graded permittivity (b) at different time.

As is shown in Fig. 6, in order to find out the influencing mechanism of graded permittivity on the surface charge, the electric field in y-direction E_y on the surface of dielectric is investigated, in which l is the distance along the dielectric barrier. The magnitude of E_y varies in a relatively narrow range on the surface of dielectric barrier with graded permittivity. This indicates that during the material surface modification process, there will be more uniform electric field distribution on the surface. Besides, when plasma approaches the surface of the dielectric barrier with graded permittivity, the volcano-shaped electric field E_y appears on the surface of dielectric barrier, forming a gradient electric field inward. The gradient electric field may result in centralized distribution of ions and electrons, making it more efficient in injection of active functional groups on the barrier surface [3] and medical application [18]. To cite this, the surface charge density is shown in Fig. 7.

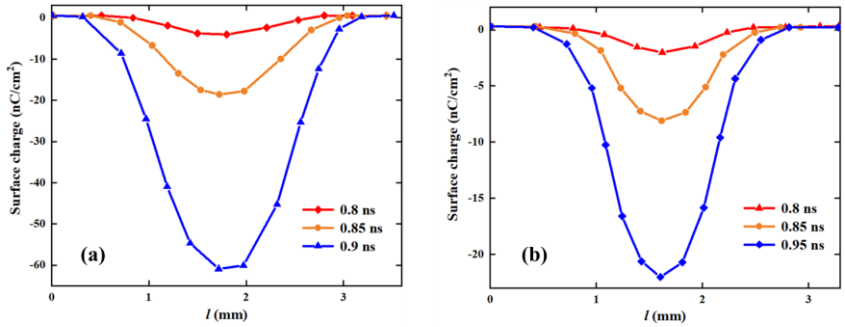

Fig. 7 – Surface charge density distribution along the dielectric with uniform permittivity (a) and graded permittivity (b) at different times during a voltage pulse.

Figure 7 depicts the surface charge density along the dielectric barrier. Comparing Fig. 7a with 7b, it can be found that the surface charge density on the dielectric barrier with graded permittivity is reduced to a much lower level, and has a relatively narrow distribution spatially. This mainly can be attributed to the electric field E_y, as shown in Fig. 6b. The movement of charged particles along the surface of the dielectric barrier is limited by the electric field strength potential, preventing it from pre-charge outside the target areas. In other words, the possibility of surface dielectric barrier discharge (SDBD) along the dielectric barrier is reduced with graded permittivity introduced.

The heavy species produced during the DBD will significantly draw attention such as O_3. In order to identify the difference of O_3 density distribution, the evolution of it is depicted in Fig. 8.

As is depicted in Fig. 8, it indicates a less number density of O_3 inside the streamer body with graded permittivity. Compared with the spatial distribution of electron density in Fig. 4, the same development trend has been maintained of both O_3 and electrons. This can be attributed to the producing sources of O_3, the reactions occurred with the consumption of electrons. The decrease of charged particle density inside the streamer body can maintain the continuous discharge process, preventing it from high power deposition on the dielectric surface or causing damage to the surface during the modification.

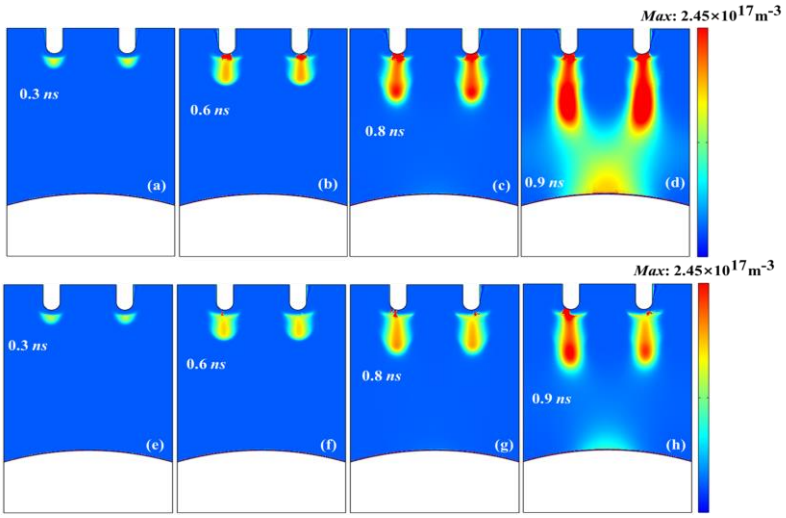

Fig. 8 – Spatial distribution of O_3 density during the propagation with uniform permittivity (a), (b), (c), (d) and graded permittivity (e), (f), (g), (h).

4. CONCLUSIONS

The following conclusions can be drawn from this study:

1) The application of twin power-electrodes can deal with considerable areas. This indicates that the arrangements of multi-electrodes will significantly change the performance of glow-like discharge in many applications such as material surface modification.

2) The electric field strength on the surface of dielectric barrier is changed into volcano-shaped distribution, and making it more central electron accumulation, inhibiting the surface discharge along the dielectric barrier outside the target areas.

3) With graded permittivity of barrier dielectric introduced, the deposition of charged particle density is much different from that with uniform permittivity barrier dielectric. It can maintain a continuous mode of plasma processing.

REFERENCES

1. I. ADAMOVICH, S.D. BAALRUD, A. BOGAERTS, P.J. BRUGGEMAN, M. CAPPELLI, V. COLOMBO, U. CZARNETZKI, U. EBERT, J.G. EDEN, P. FAVIA et al., *The 2017 Plasma Roadmap: Low temperature plasma science and technology*, Journal of Physics D: Applied Physics, **50**, *32*, art. 323001, 2017.

2. S. CHEN, T. CHENG, Z. CHEN, X. CHEN, G. ZHANG, *Multi-effects of atmospheric He/CF4 plasma jet treatment on the surface properties of epoxy resin*, Applied surface science, **544**, art. 148956, 2021.
3. L. ZHAO, W. LIU, P. LIU, J. TIAN, M. XU, S. SUN, Y. WANG, *Study on atmospheric air glow discharge plasma generation and surface modification of carbon fiber fabric*, Plasma processes and polymers, **17**, *4*, art. 1900148, 2020.
4. Y.B. GOLUBOVSKII, V.A. MAIOROV, P. LI, M. LINDMAYER, *Effect of the barrier material in a Townsend barrier discharge in nitrogen at atmospheric pressure*, Jounal of Physics D: Applied Physics, **39**, *8*, pp. 1574-1583, 2006.
5. R. LI, Q. TANG, S. YIN, T. SATO, *Investigation of dielectric barrier discharge dependence on permittivity of barrier materials*, Applied Physics Letter, **90**, *13*, art. 131502, 2007.
6. R. TSCHIERSCH, S. NEMSCHOKMICHAL, M. BOGACZYK, J. MEICHSNER, *Surface charge measurements on different dielectrics in diffuse and filamentary barrier discharges*, Journal of Physics D: Applied Physics, **50**, *10*, art. 105207, 2017.
7. G.J. ZHANG, G.Q. SU, B.P. SONG, H.B. MU, *Pulsed flashover across a solid dielectric in vacuum*, IEEE Transactions on Dielectrics and Electrical Insulation, **25**, *6*, pp. 2321-2339, 2018.
8. C. YAO, S. CHEN, G. XU, Z. CHANG, H. MU, A. SUN, G. ZHANG, *Transition from glow-like to streamer-like discharge in atmospheric pressure dielectric barrier discharge controlled by variable dielectric surface layer permittivity*, Physics of plasmas, **26**, *6*, art. 060702, 2019.
9. T. HOMOLA, R. KRUMPOLEC, M, ZEMANEK, J. KELAR, P. SYNEK, T. HODER, M. CERNAK, *An array of micro-hollow surface dielectric barrier discharges for large-area atmospheric-pressure surface treatments*, Plasma chemistry and plasma processing, **37**, *4*, pp. 1149-1163, 2017.
10. G. NAYAK, H. ABOUBAKR, S. GOYAL, P. BRUGGEMAN, *Reactive species responsible for the inactivation of feline calicivirus by a two-dimensional array of integrated coaxial microhollow dielectric barrier discharges in air*, Plasma processes and polymers, **15**, *1*, art. e1700119, 2018.
11. Z. ZHAO, W. WANG, D. YANG, X. ZHOU, H. YUAN, *Nanosecond pulsed array wire-to-wire surface dielectric barrier discharge in atmospheric air: electrical and optical emission spectra characters influenced by quantity of electrodes*, IEEE transactions on plasma science, **47**, *8*, pp. 4219-4224, 2019.
12. J. ZHANG, Y.H. WANG, D.Z. WANG, *Numerical simulation of streamer evolution in surface dielectric barrier discharge with electrode-array*, Journal of Physics D: Applied Physics, **128**, *9*, art. 093301, 2020.
13. http://www.bolsig.laplace.univ-tlse.fr/ for information about Bolsig+, accessed: February 21, 2022.
14. http://www.lxcat.net for Morgan database/ TRINITI database/ Phelps database, accessed: February 21, 2022.
15. R. MORROW, J.J. LOWKE, *Streamer propagation in air*, Journal of Physics D: Applied Physics, **30**, 4, 614, 1997.
16. T.N. TRAN, I.O. GOLOSNOY, P.L. LEWIN, G.E. GEORGHIOU, *Numerical modelling of negative discharges in air with experimental validation*, Journal of Physics D: Applied Physics, **44**, *1*, art. 015203, 2011.
17. W.S. KANG, J.M. PARK, Y. KIM, S.H. HONG, *Numerical study on influences of barrier arrangements on dielectric barrier discharge characteristics*, IEEE Transactions on Plasma Science, **31**, *4*, pp. 504-510, 2003.
18. H. CHENG, X. LIU, X. LU, D. LIU, *Active species delivered by dielectric barrier discharge filaments to bacteria biofilms on the surface of apple*, Physics of plasmas, **23**, *7*, art. 073517, 2016.

Received February 21, 2022